Journal of Solid State Chemistry 184 (2011) 1719–1725

Contents lists available at ScienceDirect

Journal of Solid State Chemistry

journal homepage: www.elsevier.com/locate/jssc

Structures, spectroscopic studies and solid-state thermal transformations of coordination polymers from P_4Se_3 and CuX (X=Cl, Br, I)

Andreas Biegerl [a], Christian Gröger [b], Hans R. Kalbitzer [b], Arno Pfitzner [a], Joachim Wachter [a,*], Richard Weihrich [a], Manfred Zabel [a]

[a] Institut für Anorganische Chemie der Universität Regensburg, 93040 Regensburg, Germany
[b] Institut für Biophysik und Physikalische Biochemie der Universität Regensburg, 93040 Regensburg, Germany

ARTICLE INFO

Article history:
Received 22 February 2011
Received in revised form
2 May 2011
Accepted 8 May 2011
Available online 14 May 2011

Keywords:
Phosphorus
Selenium
Coordination polymers
Solid-state NMR spectroscopy
Raman spectra

ABSTRACT

The formation of coordination polymers $(CuCl)P_4Se_3$ (**1**), $(CuBr)_3(P_4Se_3)_2$ (**2**), $(CuI)_3(P_4Se_3)_2$ (**3**) and $(CuI)P_4Se_3$ (**4**), from solutions of copper(I) halides and P_4Se_3 by diffusion methods has been studied. The new compounds were characterized by X-ray crystallography, solid-state ^{31}P MAS NMR and Raman spectroscopy. Theoretical studies on the DFT level in the crystalline phase allowed the unequivocal assignment of the recorded Raman shifts between 200 and 480 cm^{-1}. The structure of **1** consists of a 2D network of castellated $[CuCl]_n$ chains and bidentate P_4Se_3 molecules. The 3D network of **2** comprises $[CuBr]_n$ chains, which are linked by tridentate P_4Se_3 molecules. Compound **3** is a three-dimensional polymer composed of four-membered $(CuI)_2$ rings and castellated $[CuI]_n$ chains, which are linked by tridentate P_4Se_3 molecules involving two basal and the apical P atoms. Thermal conversion of 1 at 230 °C gives $(CuCl)_3(P_4Se_3)_2$ (**5**), which is isostructural with **2**. The thermal conversion of $(CuI)_3P_4S_3$, which was studied for comparison gave at 371 °C $(CuI)_3P_4S_4$, Cu_3PS_4 and small amounts of Cu_6PS_5I.

1. Introduction

Cage molecules like P_4Q_3 (Q=S, Se) represent a small but important class of inorganic compounds. The P_4S_3 molecule exhibits a rich coordination chemistry towards Lewis-acidic metal fragments, although addition reactions are mostly focussed at the apical and/or basal phosphorus [1]. Due to relatively poor solubility of P_4Se_3 in organic solvents there are only a few examples for P_4Se_3 [2]. Attempts to synthesize new solid-state materials containing P_4Q_3 and $(CuI)_n$ aggregates from copper(I) halides and the molten elements gave $(CuI)_3(\beta\text{-}P_4Q_4)$ (Q=S [3], Se [4,5]), while CuCl and CuBr led to decomposition reactions. We have recently found that P_4S_3 may be introduced in copper(I) halide networks by applying interdiffusion techniques from solutions of different polarity [6]. Because of the poorly developed coordination chemistry of P_4Se_3 we decided to systematically extend this work onto P_4Se_3 and CuX (X=Cl, Br, I). Herein we report the crystal structures and spectroscopic properties of the products, the calculation of Raman frequencies by DFT methods in the crystalline phase, their correlation with measured spectra and the thermally induced transformation of selected compounds.

2. Experimental

2.1. General procedure

All manipulations were carried out under nitrogen by Schlenk techniques. The diffusion experiments were carried out in Schlenk tubes of 3.0 cm diameter. P_4Se_3 was synthesized by melting red phosphorus and gray selenium in a molar ratio of 4 to 3 under a nitrogen-atmosphere, followed by extraction with CH_2Cl_2 in a Soxhlet apparatus and recrystallization from CH_2Cl_2 [7].

2.2. Syntheses

$(CuCl)P_4Se_3$ (**1**): A solution of CuCl (25 mg, 0.249 mmol) in CH_3CN (5 ml, c=49.8 mmol l^{-1}) was layered over a solution of P_4Se_3 (30 mg, 0.083 mmol) in CH_2Cl_2 (30 ml, c=2.8 mmol l^{-1}). After diffusion transparent yellow needles of **1** crystallized and were washed with CH_2Cl_2 and dried under vacuum. Anal. Calcd. for $ClCuP_4Se_3$ (459.76): Cl 7.74; Found: Cl 7.71%. ^{31}P MAS NMR (δ, ppm): 72.0 (s), −35.8 (m, $^1J_{P,Cu}$=986 Hz), −51.7 (m, $^1J_{P,Cu}$=896 Hz), −84.2 (s).

$(CuBr)_3(P_4Se_3)_2$ (**2**): A procedure similar to that for **1** was used with CuBr (36 mg, 0.249 mmol) in CH_3CN (5 ml, c=49.8 mmol l^{-1}) and P_4Se_3 (30 mg, 0.083 mmol) in CH_2Cl_2 (30 ml, c=2.8 mmol l^{-1}). Yield 78 mg (82%). ^{31}P MAS NMR (δ, ppm): 59.0 (m, $^1J_{P,Cu}$=900 Hz), −57.7 (m, $^1J_{P,Cu}$=1094 Hz), −68.1 (s), −69.8 (m, $^1J_{P,Cu}$=910 Hz).

* Corresponding author.
E-mail address: Joachim.Wachter@chemie.uni-regensburg.de (J. Wachter).

0022-4596/$ - see front matter © 2011 Elsevier Inc. All rights reserved.
doi:10.1016/j.jssc.2011.05.011

Table 1
Crystal data and structure refinements for compounds 1–4.

	1	2	3	4
Empirical formula	$ClCuP_4Se_3$	$Br_3Cu_3P_8Se_6$	$Cu_3I_3P_8Se_6$	$CuIP_4Se_3$
fw	459.76	1151.87	1292.87	551.21
Cryst. size (mm)	$0.18 \times 0.04 \times 0.01$	$0.16 \times 0.08 \times 0.03$	$0.06 \times 0.05 \times 0.02$	$0.16 \times 0.03 \times 0.01$
Cryst. system	Monoclinic	Orthorhombic	Orthorhombic	Orthorhombic
Space group	$P2_1/c$	Pnma	Pnma	Cmca
a (Å)	12.351(1)	6.447(1)	7.815(1)	7.728(1)
b (Å)	11.148(1)	27.289(1)	27.491(1)	22.618(1)
c (Å)	6.367(1)	11.331(1)	9.767(1)	10.502(1)
β (deg)	100.9(1)			
V (Å^3)	860.7(1)	1993.6(1)	2098.3(1)	1835.8(2)
Z	4	4	4	8
D_{calcd} (g cm^{-3})	3.548	3.838	4.093	3.989
μ (mm^{-1})	27.293	29.264	55.770	49.327
λ (Cu$K\alpha$, Å)	1.54184			
Instrument	Oxf. Diff. Gemini Ultra			
T (K)	123	123	123	293
Θ for data collection	5.39–62.24	3.24–62.14	4.81–62.18	3.91–51.97
Reflections collected/unique	7603/1109	12693/1427	4624/1398	5715/440
Parameters	82	94	194	48
Residual density (eÅ^{-3})	2.573/−2.106	0.884/−0.992	2.673/−1.188	1.042/−1.058
R_1, wR_2 ($I > 2\sigma$)	0.055, 0.148	0.027, 0.064	0.035, 0.084	0.045, 0.111
R_1, wR_2 (all data)	0.063, 0.156	0.032, 0.066	0.042/0.088	0.061, 0.123

$(CuI)_3(P_4Se_3)_2$ (**3**): A procedure similar to that for **1** was used with CuI (40 mg, 0.210 mmol) in CH_3CN (30 ml, c=7.0 mmol l^{-1}) and P_4Se_3 (20 mg, 0.055 mmol) in CH_2Cl_2 (25 mL, c=2.2 mmol l^{-1}). Yield 50 mg (70%).^{31}P MAS NMR (δ, ppm): 52.5 (m, $^1J_{P,Cu}$=880 Hz), −68.3 (s), −76.1 (m, $^1J_{P,Cu}$=800 Hz), −101.1 (m, $^1J_{P,Cu}$=780 Hz). Increasing the CuI concentration results in the cocrystallization of small amounts of red $(CuI)P_4Se_3$ (**4**).

2.3. Crystal structure determination

Crystallographic data of the crystal structure determinations for **1**–**5** are given in Table 1 and Table S1. The structures were solved by direct methods and refined by full-matrix least squares (SHELXL97 program) with all reflections. Further details of the crystal structure investigations may be obtained from Fachinformationszentrum Karlsruhe, 76344 Eggenstein-Leopoldshafen, Germany (fax: (+49)7247-808-666; e-mail: crysdata@fiz-karlsruhe.de, http://www.fiz-karlsruhe.de/ecid/Internet/en/DB/icsd/depot_anforderung.html) on quoting the deposition numbers CSD-422534 (**4**), -422535 (**1**), -422536 (**5**), -422537 (**2**), -422538 (**3**).

2.4. Differential thermal analysis (DTA and TG)

The DTA analyses were carried out on a Setarm TMA 92 (16.18). In each case 10–20 mg of the substances were fused into evacuated silica glass vials (diameter 0.1 cm, length 0.8 cm) and then the heat flow was recorded. The temperature range from 25 °C to 800 °C was monitored for each sample in two heating and cooling cycles (10 °C/min). Then, the thermal behavior of a new sample at the first irreversible peak was investigated. After the DTA experiment the samples were examined microscopically and by X-ray diffraction.

The TG-analyses were carried out in open Al_2O_3-cups under nitrogen-atmosphere in a temperature range of 25–600 °C with a heating rate of 10 °C/min.

2.5. Raman spectra

The Raman spectra were recorded on a Varian FTS 7000e spectrometer containing a FT Raman unit. The excitation of the microcrystalline samples was carried out with a Nd:YAG laser (λ=1064 nm) and the detection was performed with a liquid N_2 cooled Ge detector.

2.6. ^{31}P MAS NMR spectra

^{31}P MAS NMR spectra were recorded with a Bruker Avance 300 spectrometer using a double resonance 2.5 mm MAS probe. The ^{31}P resonance was 121.495 MHz. All spectra were acquired at a MAS rotation frequency of 30 kHz, a 90° pulse length of 2.3 μs and with a relaxation delay of 450 s. For spectrum simulation the program DMFIT was used [8].

2.7. Density functional theory (DFT) calculations

The calculations were performed within the framework of DFT theory as implemented in the LCAO-code CRYSTAL06 [9,10]. Therein, the electronic structure is calculated from Gaussian type local basis sets. Raman frequencies were calculated from the vibrational spectra at the gamma point [11]. Exchange and correlation were treated as described by the B3LYP functional for all results presented in this paper. All electron basis sets were used for Cu (0.28, 0.4), and Se (0.21, 1.09), valence basis sets for P (0.23, 0.49), S (0.22, 0.45), Cl (0.21, 0.38), Br (0.21, 0.36) and I (0.22, 0.33) with respective optimized coefficients for outer (sp, d) functions [12]. The calculations were converged to total energy $\Delta E < 10^{-8}$ H applying k-point shrinking factors of 4 to 8 and Anderson mixing (see [9]).

3. Results and discussion

3.1. Preparations

Layering of solutions of P_4Se_3 in CH_2Cl_2 with a solution of the respective copper halide CuX in CH_3CN (molar ratio 1:3 to 1:4) gave for X=Cl after 3 d transparent yellow needles and fine hairs of $(CuCl)P_4Se_3$ (**1**) in 83% yield. The composition was confirmed by single crystal X-ray diffraction, X-ray powder diffractometry and elemental analysis (Cl).

When the experiment was carried out with CuBr yellow-orange platelets of $(CuBr)_3(P_4Se_3)_2$ (**2**) crystallized in 82% yield.

The composition of **2** was determined by X-ray diffraction analysis, while the homogeneity was determined by means of ^{31}P MAS NMR spectroscopy (Scheme 1).

The analogous experiment with CuI gave a mixture of orange-red plates of $(CuI)_3(P_4Se_3)_2$ (**3**) and thin red prisms of $(CuI)P_4Se_3$ (**4**), which were both examined by X-ray diffraction analysis. Decreasing the concentration of CuI in acetonitrile results in a nearly selective formation of 3, the purity of which has been established by ^{31}P MAS NMR spectroscopy.

3.2. Crystal structure analysis

Compound **1** crystallizes in the monoclinic space group $P2_1/c$. The structure is composed of slightly distorted castellated $[CuCl]_n$ chains along the *c* axis, which are connected by two P_4Se_3 molecules via their phosphorus basis atoms P2 and P4 to give a two-dimensional layer (Fig. 1). The third atom of the P_3 basis (P3) and the apical atom P1 do not coordinate. The P–Se distances within the P_4Se_3 cage are comparable within experimental error with those of the free cage [13], while the distance P2–P4 is shorter by 0.03 and 0.044 Å, respectively, than the other two P–P bonds of the P_3 basis. The copper atoms are tetrahedrally surrounded by two Cl and two P atoms. The observed Cu–Cl (2.276(3)Å) and Cu–P distances (2.283(3)Å mean) are typical of copper halides and phosphides [5]. Similar $[CuCl]_n$ chains are, e.g., part of the structure of $[(CuCl)(\mu_2$-2-ethylpyrazine-N-N′$)]$ [14].

Compound **2** crystallizes in the orthorhombic space group Pnma. The structure contains two different types of castellated $[CuBr]_n$ chains, which are bridged by P_4Se_3 cages (Fig. 2). While $[Cu_1\text{-}Br_1]_n$ is planar, $[Cu_2\text{–}Br_2]_n$ is distorted along the *a* axis by 17°. As in the structure of **1** the basal atoms P2 and P4 connect two neighbored non-planar chains via Cu_2. The apical atoms P1, however, coordinate to planar chains via Cu1. The result is a 3D network, which is

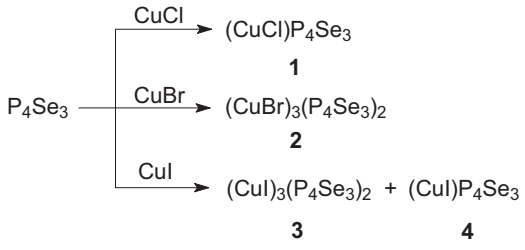

Scheme 1

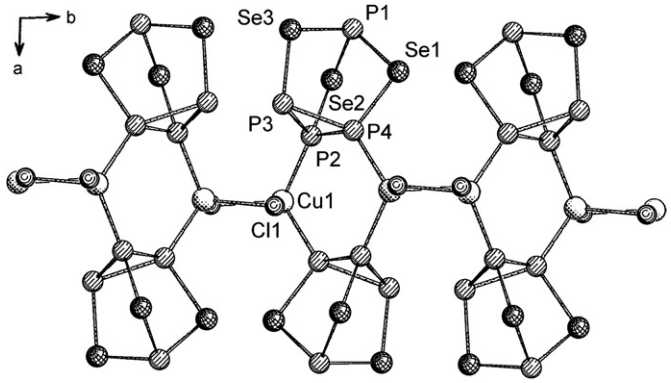

Fig. 1. Section of the 2D structure of **1**; view down the *c* axis. Selected distances (Å): Se1–P1 2.251(3), Se1–P4 2.236(3), Se2–P1 2.253(2), Se2–P2 2.235(3), Se3–P1 2.267(3), Se3–P3 2.252(2), P2–P3 2.236(3), P2–P4 2.207(3), P3–P4 2.251(3), P2–Cu1 2.276(3), P4–Cu1 2.290(3), Cu1–Cl1 2.324(3).

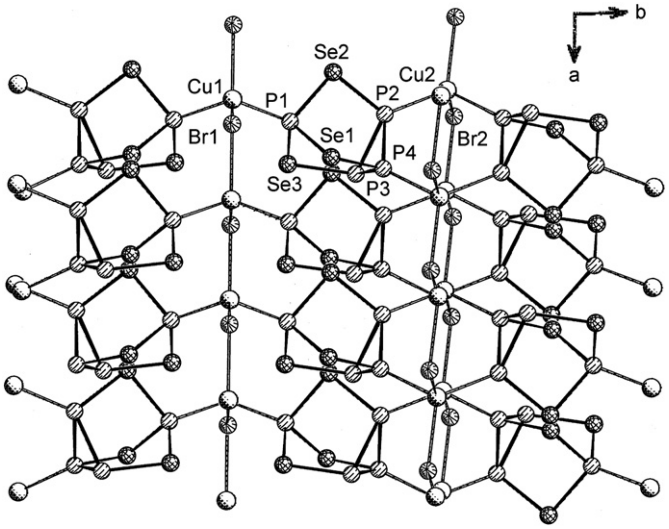

Fig. 2. Section of the 3D-structure of **2**; view down the *c* axis. Selected distances (Å): Se1–P1 2.237(2), Se1–P4 2.227(2), Se2–P1 2.248(2), Se2–P2 2.240(2), Se3–P1 2.251(2), Se3–P3 2.244(2), P2–P3 2.243(2), P2–P4 2.207(2), P3–P4 2.260(2), P1–Cu1 2.261(2), P2–Cu1(2) 2.300(2), P4–Cu1(2) 2.267(2), Cu1–Br1 2.429(2), 2.445(2), Cu_2–Br2 2.408(2), 2.448(2).

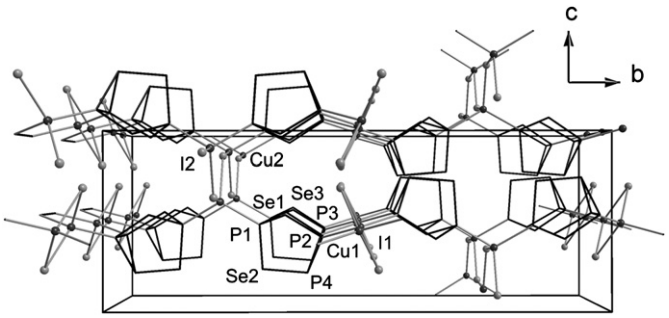

Fig. 3. Section of the 3D-structure of **3**; view along the *a* axis. Selected distances (Å): Se1–P1 2.245(2), Se1–P3 2.238(2), Se2–P1 2.245(2), Se2–P4 2.253(2), Se3–P1 2.237(2), Se3–P2 2.232(2), P2–P3 2.217(3), P2–P4 2.255(3), P3–P4 2.262(3), Cu1–P2 2.287(2), Cu1–P3 2.287(2), Cu_2–P1 2.263(2), Cu1–I1 (mean) 2.612(2), Cu_2–I2 (mean) 2.641(2), Cu1–Cu1a 3.115(2).

isostructural with $(CuCl)_3(P_4S_3)_2$ [6a]. The Cu–Br distances range from 2.408(1) to 2.448(1)Å and the Cu–P distances from 2.261(1) to 2.267(1)Å. Each copper atom of the respective chains is tetrahedrally surrounded by two P and two Br atoms with angles between 103.6(1) and 117.9(1)°. The distance P3–P4 is slightly longer by 0.03 Å than the other two ones within the P_3 basis. $[CuBr]_n$ chains similar to that in **1** and **2** have been found in coordination polymers of the type $[(CuBr)_2$(triazine)$]$ [15].

Compound **3** crystallizes in the orthorhombic space group Pnma. The structure is built up of castellated $[CuI]_n$ chains with each copper (Cu_2) bearing a pair of apically (P1) coordinated P_4Se_3 cages. The backsides of the cages are bridged by planar Cu_2I_2 four-membered rings while the third basal P atom (P4) remains uncoordinated. As a result an unprecedented three-dimensional structure is formed (Fig. 3). The bond parameters of the P_4Se_3 cage behave similarly to those of **1** and **2**.

Compound $(CuI)P_4Se_3$ (**4**) crystallizes in the orthorhombic space group Cmca. Like its isostructural analog $(CuI)P_4S_3$ [6] the structure is a one-dimensional polymer containing planar $(CuI)_2$ four-membered rings bridged by P_4Se_3 units (Fig. S1). The atoms P1 (apical) and P2 (basal) are not coordinated.

A comparison of the crystal structures found in the P_4Se_3/CuX system (X=Cl, Br, I) with those of P_4S_3/CuX polymers reveals as common features copper halide substructures consisting of planar Cu_2X_2 four-membered rings (X=Br, I) and/or castellated $[CuX]_n$ chains. As a result one-dimensional ribbons (**4**), or two- (**1**) and three-dimensional networks (**2**, **3**) are formed, which are new structure types in the case of **1** and **3**. It is striking that no hexagonal $(CuX)_n$ substructures are formed, which seem to be typical of P_4S_3 containing polymers [6].

3.3. ^{31}P MAS NMR spectroscopy

More structural informations on the polymers **1**–**4** may be obtained by solid-state ^{31}P MAS NMR spectroscopy and by comparison with the spectrum of α-P_4Se_3, which was also recorded. For the latter resonance signals for the apical P atom at $\delta=81.2$ and 77.2 ppm and for the basal P atoms at $\delta=-67.0$ ppm were found with an approximate $^{31}P_{apical}$:$^{31}P_{basal}$ integral ratio of 1:3 (Fig. S2). The splitting of the signal of the apical P atom into two singlets may be explained by the packing of the cage molecules in the unit cell [13]. A similar splitting was reported for α-P_4S_3 [16].

The ^{31}P MAS NMR spectrum of **1** exhibits two groups of signals centered at $\delta=57$ and -60 ppm (Fig. 4). The singlet at $\delta=72.0$ ppm may be assigned to apical P1. The broad signal at $\delta=-60$ ppm has been shown by simulation to be the result of the superposition of one singlet at $\delta=-84.2$ ppm and two multiplets at $\delta=-35.8$ ($J_{P,Cu}=986$ Hz) and -51.7 ppm ($J_{P,Cu}=896$ Hz). The latter indicate coupling of magnetically inequivalent basis atoms P2 and P4 with $^{63/65}Cu$, whereas the singlet may be assigned to the uncoordinated atom P3 of the P_3 basis. ^{31}P–^{77}Se coupling was not observed.

The ^{31}P MAS NMR spectrum of **2** exhibits two groups of signals (Fig. 5). Simulation of the spectrum reveals a multiplet at $\delta=59.0$ ppm ($J_{P,Cu}=900$ Hz), a singlet at $\delta=-68.1$ ppm and two multiplets at $\delta=-57.7$ ppm ($J_{P,Cu}=1094$ Hz) and $\delta=-69.8$ ppm ($J_{P,Cu}=910$ Hz), respectively. The overall pattern is in agreement with the structure of **2** (Fig. 2). The magnetical inequivalence of the atoms P2 and P4 indicates that the symmetry of the free cage (C_{3v}) is lowered by coordination (C_1).

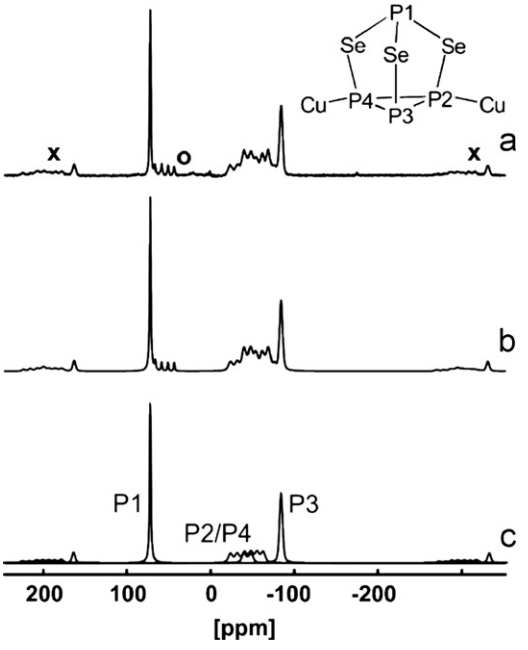

Fig. 4. ^{31}P MAS NMR spectrum of **1**: (a) experimental spectrum; (b) simulated spectrum; (c) simulated spectrum showing individual components. Spinning side bands are marked by the symbol $\times$, impurities by $\circ$.

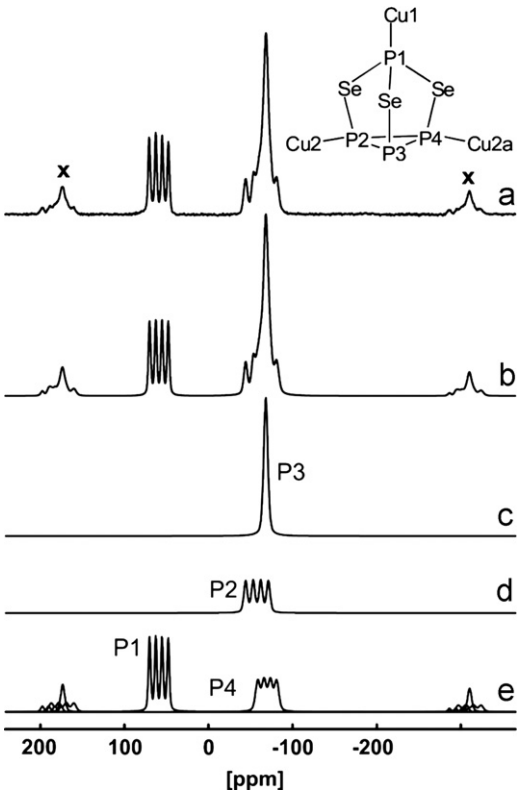

Fig. 5. ^{31}P MAS NMR spectrum of **2**: (a) experimental spectrum; (b) simulated spectrum; (c–e) simulated spectra showing individual components. Spinning side bands are marked by the symbol $\times$.

According to X-ray powder diffraction compound **3** is contaminated by compound **4**. A nearly pure sample of **3** was obtained employing a low concentration of CuI in acetonitrile. The resulting ^{31}P MAS NMR spectrum shows two groups of signals (Fig. 6). Simulation of the spectrum reveals a multiplet at $\delta=52.5$ ppm $J(_{P,Cu}=880$ Hz). The high field signal splits into two multiplets (copper coordination of P2 and P3) at $\delta=-76.1$ ppm ($J_{P,Cu}=800$ Hz) and -101.1 ppm ($J_{P,Cu}=780$ Hz), respectively, and a singlet at $\delta=-68.3$ ppm. The latter may be assigned to P4 of the P_3 basis. Overall, the spectrum of **3** is in agreement with the crystal structure and it is similar to that of **2** inspite of different CuX substructures.

The ^{31}P MAS NMR spectrum of a mixture of **3** and **4** allows a clear identification of an additional singlet at $\delta=91.3$ ppm, which may be assigned to the apical P atom of **4**. The other resonances of **4** are superposed by those of **3**. It is striking that the resonance of the apical P atom is downfield shifted compared to α-P_4Se_3 (Table 2). A similar effect was observed for the apical resonances of the isostructural polymers $(CuX)P_4S_3$ (X=Br, I) [6]. Ab initio calculations have shown that possible explanations have to take into account electronic effects rather than steric arguments [17].

A detailed ^{31}P MAS NMR spectroscopic investigation of $(CuI)_3(\beta$-$P_4Q_4)$ polymers (Q=S, Se) has been published recently [4]. In all cases it was found that the coordination of Cu(I) at phosphorus gave rise to a high field shift of the resonance signal by about 50 ppm compared to the free cage molecule, whereas the signals of uncoordinated P atoms were only slightly affected. These effects were explained by Cu–P back donation and electronic perturbations by Cu^+ complexation, which are predominantly local and mostly confined to the directly Cu-bonded

P-atoms [4]. A similar but less pronounced trend is found for the chemical shifts of **1**–**3**, except the resonances of P2/P4 (**1**), P2 (**2**) and the apical P atom of **4** (Table 2).

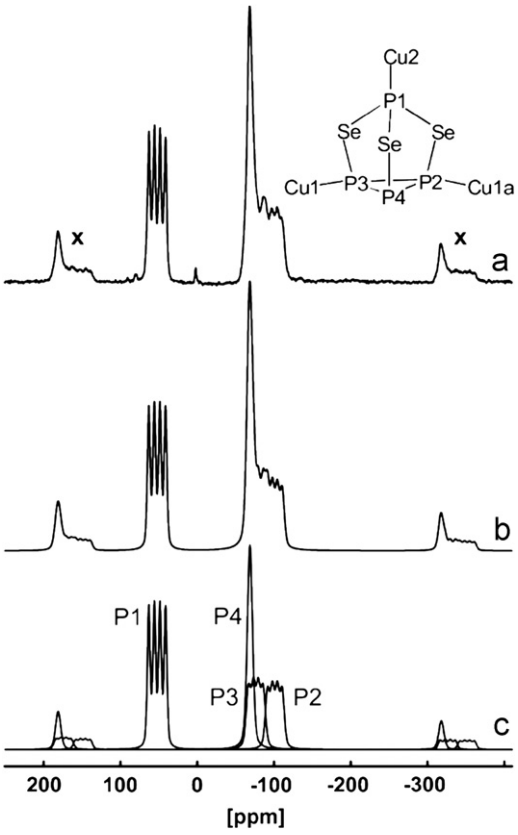

Fig. 6. ^{31}P MAS NMR spectrum of **3**: (a) experimental spectrum; (b) simulated spectrum; (c) simulated spectrum showing individual components. Spinning side bands are marked by the symbol ×.

Table 2
^{31}P MAS NMR chemical shifts in δ(ppm) and coupling constants ^{31}P–$^{63/65}$Cu in J (Hz) of P_4Se_3 and compounds 1–4.

	P_{apical}	P_{basal}
α-P_4Se_3	81.2, 77.2	−67
(CuCl)P_4Se_3 (1)	72.0	−35.8 (9 8 6), −51.7 (896), −84.2
$(CuBr)_3(P_4Se_3)_2$ (2)	59.0 (900)	−57.7 (1094), −68.1, −69.8 (910)
$(CuI)_3(P_4Se_3)_2$ (3)	52.5 (880)	−68.3, −76.1 (800), −101.1 (780)
(CuI)P_4Se_3 (4)	91.3	[a]

[a] Superposed multiplet.

3.4. Theoretical and Raman spectroscopic investigations

Recently, we have studied the nature of the interaction between P_4S_3 and copper(I) halides in periodic structures by density functional theory (DFT) calculations. The use of the program package CRYSTAL06 [9] allowed to consider the influence of packing effects and intermolecular forces in the condensed phase. The DFT approach was successfully applied to calculate vibrational frequencies as stated by comparison with Raman spectra [17].

Computational studies of frequencies of crystalline P_4Se_3 were carried out using the same basis set for phosphorus as in the computation of the Raman modes of P_4S_3. The basis set of selenium was optimized by calculation of the cage geometry and by correlation of calculated and measured Raman modes. The visualization of the vibration modes by the program Jmol [18] allowed an unambiguous assignment. The calculated P–P distances of the P_3 basis deviate by 2%, while the other calculated distances come close to the experimental values [13]. The Raman modes and the corresponding vibrational assignments of P_4Se_3 have already been calculated for the gas phase (Table 3) [19]. Computational studies of frequencies of crystalline P_4Se_3 show a better agreement with experimental Raman shifts. The introduction of scaling factors is not necessary.

A comparison of experimental Raman spectra of P_4Se_3 and **1** is shown in Fig. 7. The observed Raman modes ν_1, ν_2 and ν_6 may be assigned to the vibrations P–Se–P_{wag}, P–Se–P_{bend} and Se–$P_{stretch}$. The intense ν_4, ν_3 and ν_5 modes, which are all typical of the free cage were split into a couple of Raman active frequencies

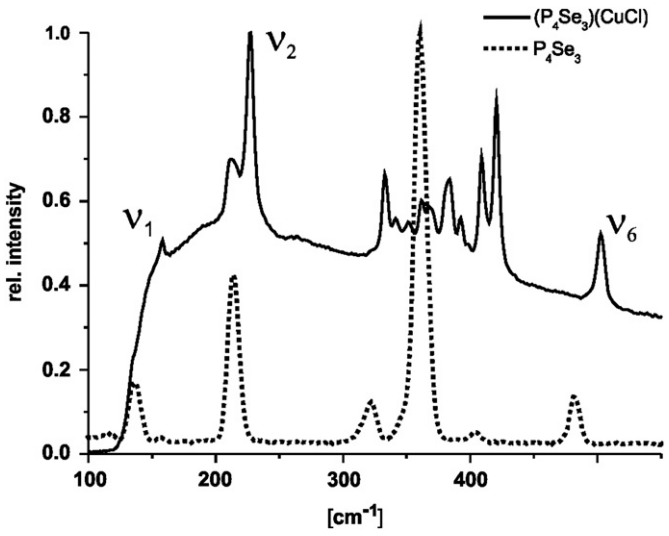

Fig. 7. Raman spectra of P_4Se_3 and (CuCl)P_4Se_3 (**1**).

Table 3
Comparison of Raman shifts (cm^{-1}) of P_4Se_3 calculated in the gas phase and in the condensed phase (CRYSTAL06) and of 1 and 3 with experimental shifts.

P_4Se_3			**1**		**3**		Assignment
SQM-method[a]	DFT/B3LYP[b]	Exp. Raman shift	Calcd.	Exp.	Calcd.	Exp.	
168	161	131	152	158	145	157	ν_1, P–Se–P_{wag}
269	187	209	211	226	216	226	ν_2, P–Se–P_{bend}
404	286	317	–	–	–	–	ν_3, P–$P_{stretch}$
442	351	355	–	–	350	353	ν_4, P–Se–$P_{stretch\ (s)}$
484	380	397	–	–	406	414	ν_5, P–Se–$P_{stretch\ (a)}$
561	468	477	476	503	492	495	ν_6, Se–$P_{stretch}$

[a] Scaled quantum mechanical calculations [19].
[b] Condensed phase, this work.

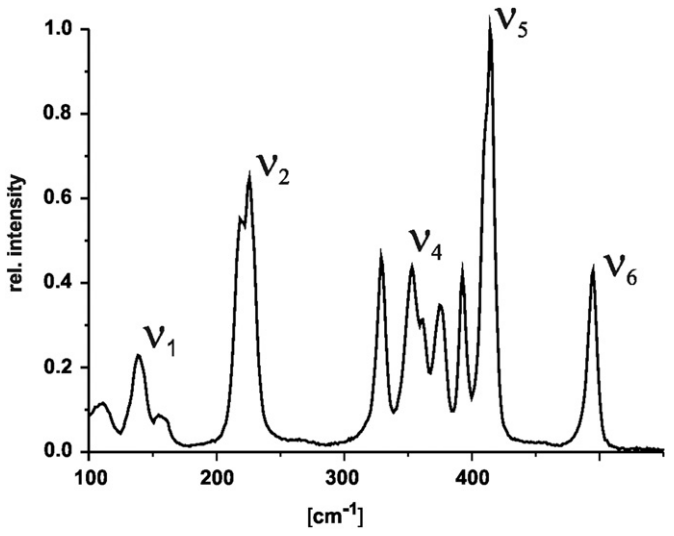

Fig. 8. Raman spectrum of $(CuI)_3(P_4Se_3)_2$ (**3**).

between 320 and 420 cm^{-1} as a consequence of symmetry reduction. The frequencies ν_1, ν_2 and ν_6 are also affected by coordination as shown by significant shifts to higher wave numbers when compared to free P_4Se_3 (Table 3).

The Raman spectrum of **3** (Fig. 8) is similar to that of **1**. This implies that the modes ν_1, ν_2 and ν_6 exhibit nearly the same red shift with respect to P_4Se_3 (Table 3). The frequencies between 330 and 420 cm^{-1} are difficult to assign except the mode ν_4 at 353 cm^{-1}, which can be assigned to symmetrical P–Se–$P_{stretch}$. This vibration is not affected by Cu coordination of the cage, while ν_5 is shifted by 18 cm^{-1} to red.

3.5. Investigation of thermally induced solid-state transformation reactions

3.5.1. Thermal conversion of $(CuCl)P_4Se_3$ (**1**) and $(CuBr)_3(P_4Se_3)_2$ (**2**)

The preparation of $(CuI)_3(\beta\text{-}P_4Q_4)$ (Q=S, Se) was carried out at high temperatures starting from the elements and CuI [3]. Therefore, it seems interesting to investigate the thermal behavior of compounds with already preformed building blocks like in **1** or **2**, which are both available in pure form. For comparison purposes the thermal behavior of previously prepared $(CuI)_3P_4S_3$ [6a] has also been studied.

The TG spectrum of **1** is in agreement with the formation of PCl_3 as a decomposition product. The corresponding DTA diagram of **1** shows two irreversible endothermic peaks at 221 and 255 °C, respectively. Therefore, 150 mg of pure **1** were sealed in a silica glass vial and annealed at 230 °C for three days. After slow cooling of the sample red-brown prisms were obtained, which were analyzed by single crystal X-ray diffraction and ^{31}P MAS NMR spectroscopy. According to these studies an optically homogenous product of composition $(CuCl)_3(P_4Se_3)_2$ (**5**) has formed. The compound is isostructural with **2**, but with two kinds of $[CuCl]_n$ chains instead of $[CuBr]_n$ chains (Fig. S3, Tables S1 andS2). This implies release of P_4Se_3 and a structural reorganization from two- to three-dimensional network.

The ^{31}P MAS NMR spectrum of **5** proves the homogeneity of the sample and it is in agreement with the crystal structure (Fig. 9). It shows a multiplet at δ=55.3 ppm ($^1J_{P,Cu}$=945 Hz), which may be assigned to apical P1 of the cage and a group of signals, which is composed of two multiplets at δ=−56.0 ($^1J_{P,Cu}$=1081 Hz) and −74.4 ppm ($^1J_{P,Cu}$=751 Hz). These indicate magnetical inequivalence of P2 and P4. The singlet at δ=−68.3 ppm comes from the uncoordinated basal atom P3.

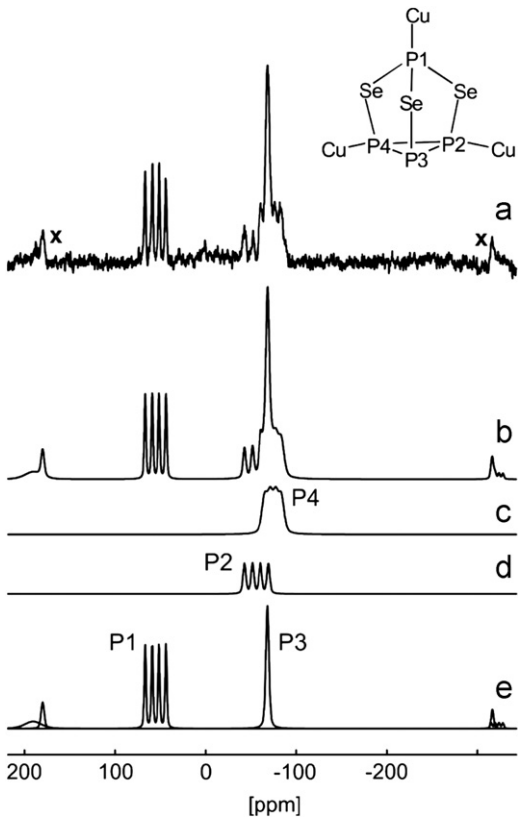

Fig. 9. ^{31}P MAS NMR spectrum of annealed **1**: (a) experimental spectrum; (b) simulated spectrum of **5**; (c–e) simulated spectra showing individual components. Spinning side bands are marked by the symbol ×.

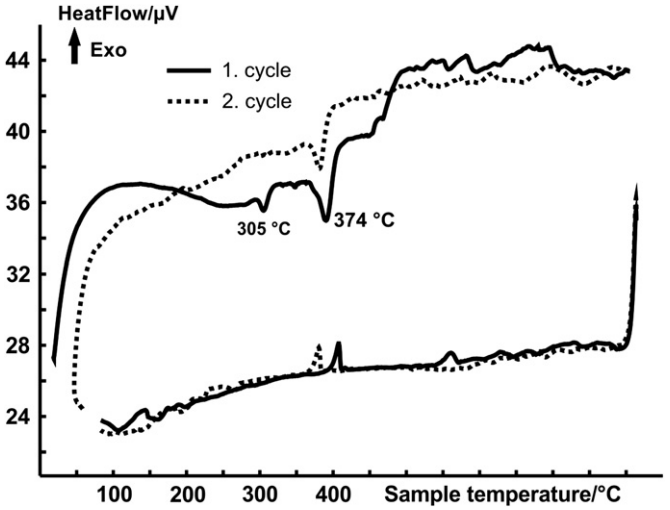

Fig. 10. DTA diagram of $(CuI)_3P_4S_3$ between 25 and 800 °C (heating rate: 10 °C/min).

Annealing of $(CuBr)_3(P_4Se_3)_2$ (**2**) at 320 °C for 3 d gave a dark shining product. X-ray diffraction experiments showed it to be amorphous and ^{31}P NMR MAS spectroscopy could not be applied successfully.

3.5.2. Thermal conversion of $(CuI)_3P_4S_3$

For the purpose of comparison the DTA diagram of $(CuI)_3P_4S_3$ [6a] has been recorded. On heating the compound in a DTA

experiment between 25 and 800 °C an irreversible peak at 297 °C and a reversible endothermic peak at 374 °C were observed (Fig. 10). To get further insight into this thermal reaction 250 mg of the pure compound were sealed in an ampoule and annealed for 11 d at 371 °C. After slow cooling black shining crystals and yellow platelets were found by microscopic investigation.

An X-ray diffraction analysis of the black microcrystals gave cell data, which were identical with those of Cu_6PS_5I [20]. This compound is a member of the argyrodite family Cu_6PQ_5X (Q=S, Se; X=Cl, Br, I), which can be directly synthesized from the elements and the appropriate copper halide. The yellow crystals were determined as Cu_3PS_4, in which tetrathiophosphate ions coordinate at copper cations in a tetrahedral manner [21]. The ^{31}P MAS NMR spectrum reveals two multiplets at $\delta=145.4$ ppm ($^1J_{P,Cu}=1212$ Hz) and $\delta=118.2$ ppm ($^1J_{P,Cu}=1217$ Hz) and one singlet at $\delta=84.1$ ppm (Fig. S4). This pattern is in good agreement with that of $(CuI)_3P_4S_4$ [3a]. Unfortunately, a crystallographic evidence for this compound could not be found. On the other hand, the resonances of Cu_3PS_4 and of Cu_6PS_5I ($\delta=78.3$ ppm, taken from a freshly prepared sample) may be covered by the signal at 84.1 ppm.

4. Conclusions

The formation and structural characterization of coordination polymers from P_4Se_3 and copper(I) halide building blocks from solution has been described. The results extend the poorly developed coordination chemistry of the P_4Se_3 cage and even differences are found compared to the structures of related CuX polymers containing P_4S_3 units as linkers. For the first time the thermal behavior of selected $(CuX)_m(P_4Q_3)_n$ coordination polymers has been studied showing unexpected thermally induced transformations in the solid-state.

Supporting Information

Structure of **4** (Fig. S1), ^{31}P MAS NMR spectrum of α-P_4Se_3 (Fig. S2), structure of **5** (Fig. S3), ^{31}P MAS NMR spectrum of annealed $(CuI)_3(P_4S_3)$ (Fig. S4) and crystallographic data of **5** (Tables S1 and S2).

Acknowledgment

This work was supported by the Deutsche Forschungsgemeinschaft (Wa 486/11-1 and We 4284/1-1). We gratefully acknowledge continuous support by Prof. Dr. M. Scheer. R.W. thanks Prof. R. Dovesi for fruitful discussions. We also thank Dr. M. Schlosser for recording the Raman spectra.

Appendix A. Supporting information

Supplementary data associated with this article can be found in the online version at doi:10.1016/j.jssc.2011.05.011.

References

[1] Complexes of P4S3 with Lewis-acidic metal fragments are summarized in J. Wachter, Coord. Chem. Rev. 254 (2010) 2078.
[2] (a) H. Nowottnick, K. Stumpf, R. Blachnik, H. Reuter, Z. Anorg. Allg. Chem. 625 (1999) 693;
(b) C. Aubauer, E. Irran, T.M. Klapötke, W. Schnick, A. Schulz, J. Senker, Inorg. Chem. 40 (2001) 4956;
(c) M. di Vaira, I. de los Rios, F. Mani, M. Peruzzini, P. Stoppioni, Eur. J. Inorg. Chem. (2004) 293;
I. de los Rios, F. Mani, M. Peruzzini, P. Stoppioni, J. Organomet. Chem. 689 (2004) 164.
[3] (a) S. Reiser, G. Brunklaus, J.H. Hong, J.C.C. Chan, H. Eckert, A. Pfitzner, Chem. Eur. J. 8 (2002) 4228;
(b) A. Pfitzner, S. Reiser, H.-J. Deiseroth, Z. Anorg. Allg. Chem. 625 (1999) 2196;
(c) A. Pfitzner, S. Reiser, Inorg. Chem. 38 (1999) 2451.
[4] G. Brunklaus, J.C.C. Chan, H. Eckert, S. Reiser, T. Nilges, A. Pfitzner, Phys. Chem. Chem. Phys. 5 (2003) 3768.
[5] A. Pfitzner, Chem. Eur. J. 6 (2000) 1891.
[6] (a) A. Biegerl, E. Brunner, C. Gröger, M. Scheer, J. Wachter, M. Zabel, Chem. Eur. J. 13 (2007) 9270;
(b) A. Biegerl, C. Gröger, H.R. Kalbitzer, J. Wachter, M. Zabel, Z. Anorg. Allg. Chem. 636 (2010) 770.
[7] A. Stock, Ber. Dtsch. Chem. Ges. 43 (1910) 150.
[8] D. Massiot, F. Fayon, M. Capron, I. King, S. Le Calve, B. Alonso, J.-O. Durand, B. Bujoli, Z. Gan, G. Hoatson, Magn. Reson. Chem. 40 (2002) 70.
[9] R. Dovesi, V.R. Saunders, C. Roetti, R. Orlando, C.M. Zicovich-Wilson, F. Pascale, B. Civalleri, K. Doll, N.M. Harrison, I.J. Bush, P. D'Arco, M. Llunell, CRYSTAL06, User's Guide, Torino (2006).
[10] M.D. Towler, M. Causa, A. Zupan, Comput. Phys. Commun. 98 (1996) 181.
[11] F. Pascale, C.M. Zicovich-Wilson, F. Lopez Gejo, R. Civalleri, R. Orlando, R. Dovesi, J. Comput. Chem. 25 (2004) 888.
[12] Crystal basis set library: 〈http://www.crystal.unito.it/Basis_Sets/Ptable.html〉.
[13] (a) J.R. Rollo, G.R. Burns, W.T. Robinson, R.J.H. Clark, H.M. Dawes, M.B. Hursthouse, Inorg. Chem. 29 (1990) 2889;
(b) A. Sergi, M. Ferrario, S.R. Elliott, I.R. McDonald, Mol. Phys. 84 (1995) 727.
[14] C. Näther, I. Jeß, J. Solid State Chem. 169 (2002) 103.
[15] A.J. Blake, N.R. Brooks, N.R. Champness, P.A. Cooke, A.M. Deveson, D. Fenske, P. Hubberstey, W.-S. Li, M. Schröder, J. Chem. Soc., Dalton Trans. (1999) 2103.
[16] I. Raabe, S. Antonijevic, I. Krossing, Chem. Eur. J. 13 (2007) 7510.
[17] G. Balazs, A. Biegerl, C. Gröger, J. Wachter, R. Weihrich, M. Zabel, Eur. J. Inorg. Chem. (2010) 1231.
[18] Jmol: an open-source Java viewer for chemical structures in 3D. 〈http://www.jmol.org/〉.
[19] M. Ystenes, F. Menzel, W. Brockner, Spectrochim. Acta Part. A—Mol. Biomol. Spectrosc. 50 (1994) 225.
[20] T. Nilges, A. Pfitzner, Z. Kristallogr. 220 (2005) 281.
[21] A. Pfitzner, S. Reiser, Z. Kristallogr. 217 (2002) 1.